

# Internal Rotation and Intermolecular Vibrations of the Phenol–Methanol Cluster: A Comparison of Spectroscopic Results and Ab Initio Theory

Ch. Plützer, Ch. Jacoby, and M. Schmitt\*

Heinrich-Heine-Universität Düsseldorf, Institut für Physikalische Chemie und Elektrochemie I, Universitätsstrasse 26.43.02, D-40225 Düsseldorf, Germany

Received: April 17, 2001; In Final Form: October 31, 2001

The vibronic spectra of five deuterated species of the binary phenol–methanol cluster are compared to the intermolecular vibrational frequencies of an ab initio-based normal-mode analysis. Isotopomers with equal mass could be distinguished experimentally using spectral hole-burning spectroscopy. The vibronic bands of phenol–methanol are split into A and E components because of the internal rotation of the methyl group. This torsional splitting is increased for three of the intermolecular vibrations because of coupling to the large-amplitude motion. Guided by comparison to an ab initio normal-mode analysis and by the torsional splitting of some of the vibronic bands, a complete intermolecular vibrational assignment for the phenol–methanol cluster is presented.

## I. Introduction

Clusters of phenol with methanol represent an interesting model system to study the influence of the sensitive equilibrium between hydrogen bonding and van der Waals interactions on the cluster structure. The binary cluster of phenol with methanol has been studied in detail both experimentally and theoretically.<sup>1–8</sup>

For the phenol–methanol cluster, vibrational frequencies for the electronic ground state have been determined using dispersed fluorescence spectroscopy. The frequencies of a bending mode and of the stretching mode were determined to be 22 and 162  $\text{cm}^{-1}$ , respectively, by Abe et al.<sup>2</sup> In the fluorescence excitation spectrum of the  $S_1$  state, this group<sup>1</sup> observed vibronic bands at 27 and 175  $\text{cm}^{-1}$  that they assigned to the corresponding transitions in the  $S_1$  state.

Only one conformer of the phenol–methanol cluster is responsible for absorption in the observed spectral region; this conformer has been confirmed using spectral hole-burning fluorescence spectroscopy (SHB)<sup>5</sup> with analysis of the electronic origin of phenol–methanol. From SHB and dispersed fluorescence measurements, the six intermolecular vibrations both in the  $S_0$  and  $S_1$  states could be assigned. Recently, Stahl<sup>9</sup> took a Fourier transform microwave spectrum of the phenol–methanol cluster, yielding rotational and centrifugal constants for the electronic ground state.

In two preceding publications, we described the determination of the structure of the phenol–methanol cluster by rotationally resolved UV spectroscopy,<sup>7,8</sup> assisted by ab initio calculations. Because of the torsional motion of the methyl group, the vibronic origin is split into A and E subbands. The evaluation of both torsional bands yielded rotational barriers for the electronic ground and excited states.

An ab initio analysis of the intermolecular vibrations in the electronic ground state has been published by Gerhards et al.<sup>4</sup> Their calculations at the Hartree–Fock level predicted a translinear geometry, as in the case of the phenol–water cluster. Courty et al. present a different structure of the cluster on the

basis of a semiempirical model potential.<sup>6</sup> In their structure, the C–O bond of the methanol moiety is nearly perpendicular to the aromatic ring. This structure is very similar to that determined from rotationally resolved LIF spectroscopy in our group.<sup>7</sup>

Although the structure of the phenol–methanol cluster can be reproduced at the MP2 level of theory even with moderate basis sets, the intermolecular vibrational frequencies obtained at this level of theory show a large deviation from the experimental ones. Therefore, we performed R2PI and SHB measurements for five differently deuterated clusters to obtain straightforward assignments of the intermolecular vibrations in the electronically excited state.

## II. Computational Methods

All ab initio calculations were performed using the Gaussian 98 program package.<sup>10</sup> The SCF convergence criterion used for our calculations was an energy change below  $10^{-8}$  hartree, whereas the convergence criterion for the gradient optimization of the molecular geometry was  $\partial E/r < 1.5 \times 10^{-5}$  hartree/bohr and  $\partial E/\partial\varphi < 1.5 \times 10^{-5}$  hartree/degree, respectively. The structure optimizations for the electronic ground state have been performed at the HF and MP2 levels of theory. A normal-mode analysis has been performed using the analytical second derivatives of the potential energy surface to obtain the intermolecular vibrational frequencies for the different isotopically substituted clusters.

The potential energy surface along two intermolecular coordinates has been calculated at the MP2/6-31G(d,p) level of theory using redundant internal coordinates. The energy has been calculated in increments of  $10^\circ$  for the internal rotation angle and for the librational angle (cf. chapter IVB) while all other internal coordinates have been kept at their equilibrium values.

The intermolecular vibrational frequencies of the first excited singlet state have been calculated with the CIS method using Pople's 6-31G(d,p) basis set. Although the CIS method is based on the HF determinant and does not include dynamical electron

\* To whom correspondence should be addressed. E-mail: mschmitt@uni-duesseldorf.de.

correlation, quite reliable results for the geometry optimization of electronically excited states of various molecules have been obtained.<sup>11</sup> Because the description of clusters in the electronic ground state required the inclusion of dynamical electron correlation, reliable results for the  $S_1$  state can only be expected using correlated methods such as CASPT2. To describe the investigated effects would require an active space that is currently too large to allow these calculations.

### III. Experimental Section

The experimental setup for the resonance-enhanced two-photon ionization (R2PI) and UV–UV spectral hole burning (SHB) is described in detail elsewhere.<sup>12,13</sup> Briefly, the vacuum apparatus consists of a source chamber in which the molecular beam is formed by expanding a mixture of helium, phenol, and methanol through the 300- $\mu\text{m}$  orifice of a pulsed nozzle (General Valve, Iota One). Phenol was kept at room temperature, whereas methanol was cooled to  $-20^\circ\text{C}$  using a Peltier cooler to reduce the formation of larger clusters. Deuterated phenol has been prepared by refluxing phenol (Riedel de Hen, p.A.) with  $\text{D}_2\text{O}$  for 2 h, evaporating the solvent, and repeating this procedure four times.  $\text{CD}_3\text{OD}$  and  $\text{CD}_3\text{OH}$  were purchased from Chemotrade ( $\text{D} \geq 99.5\%$ ). The skimmed molecular beam (Beam Dynamics Skimmer, 1-mm orifice) crosses the laser beams at right angles in the ionization chamber. The ions are extracted in a gridless Wiley–McLaren-type time-of-flight (TOF) spectrometer (Bergmann Messgerate Entwicklung) that is perpendicular to the molecular beam and laser direction; the ions enter the third (drift) chamber where they are detected using multi-channel plates. The vacuum in the three chambers with the molecular beam on was  $1 \times 10^{-3}$  mbar (source),  $5 \times 10^{-5}$  mbar (ionization), and  $1 \times 10^{-7}$  mbar (drift). The resulting TOF signal was digitized by a 500-MHz oscilloscope (TDS 520A, Tektronix) and transferred to a personal computer, where the TOF spectrum was recorded and stored.

The R2PI measurements were carried out using the frequency-doubled output of an Nd/YAG (Spectra Physics, GCR170) pumped dye laser (LAS, LDL205) operated with Fluorescein 27. For hole-burning spectroscopy, the second harmonic of an Nd/YAG (Spectra Physics GCR3) pumped dye laser (LAS, LDL205) operated with Fluorescein 27 was used. Both lasers were calibrated by comparison with the tabulated transition frequencies of the iodine spectrum. The ions formed by the hole-burning laser, which fires 800 ns before the probe laser fires, are rejected by a permanent extraction field of  $-250$  V in the acceleration region, which accelerates the burn-laser ions onto the repeller plate. One hundred nanoseconds before the probe laser fires, the field is switched for 500 ns to  $+2200$  V by a fast push–pull high-voltage switch (Behlke) to transmit the probe-laser ions to the detector.

The apparatus used for dispersed fluorescence spectroscopy consists of a high-vacuum chamber and a pulsed nozzle (General Valve Iota One 300- $\mu\text{m}$  nozzle hole). The vacuum is maintained by a 2000  $\text{L s}^{-1}$  oil diffusion pump (Edwards), backed by a rotary pump (Leybold D65B). Pressures were  $1 \times 10^{-6}$  (beam off) and  $5 \times 10^{-4}$  mbar (beam on). The molecular beam is crossed at right angles with the output of an excimer (Lambda Physik LPX 100) pumped, frequency-doubled dye laser (Lambda Physik FL 2002). The emitted fluorescence is collected and focused by a two-lens system on the entrance slit of a 1-m Czerny–Turner monochromator with an aperture of  $f/8.4$  (Jobin Yvon THR 1000). We used a holographic grating (11  $\text{cm} \times 11$  cm) in second grating order with 2400 grooves/mm. The fluorescence is imaged onto the photocathode of the CCD

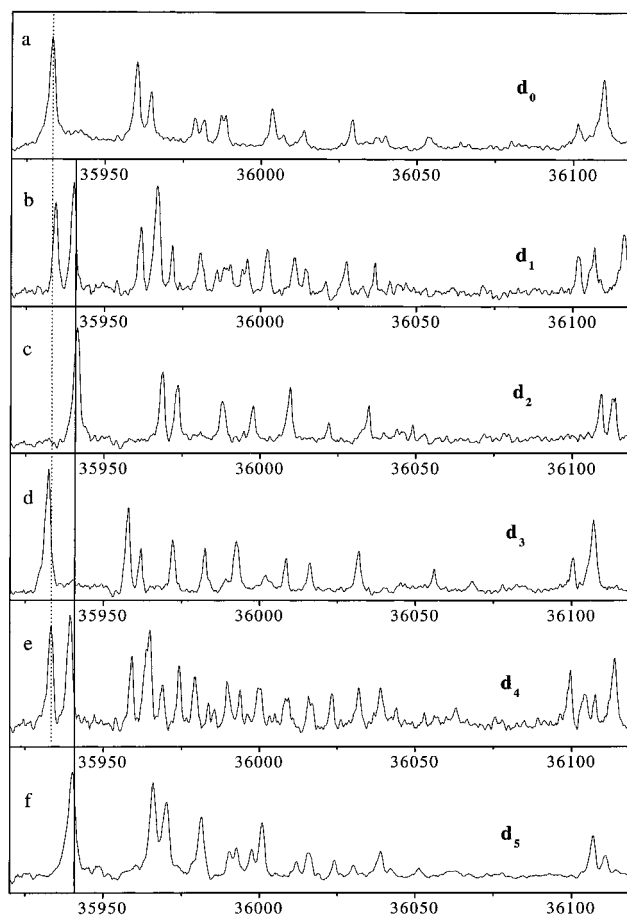


**Figure 1.** R2PI spectra of  $d_0$ - to  $d_5$ -phenol–methanol in the region of the intermolecular vibrations. The  $d_1$  and  $d_4$  mass traces show vibronic bands due to two different isotopomers. Relative accuracy of band positions:  $0.2 \text{ cm}^{-1}$ .

camera, intensified, and recorded on the CCD chip after a 15/25 reduction of the image size in an optical fiber taper. The dispersed fluorescence is recorded with 12 bit resolution by the intensified slow-scan, gated CCD camera (LaVision, Flame Star) positioned in the image plane of the monochromator.

### IV. Results and Discussion

**A. Distinction of the Isotopomers.** Figure 1 shows the R2PI spectra of the examined deuterated species of the binary phenol–methanol cluster. A mixture of the isotopomers of the cluster has been produced by mixing phenol,  $d_1$ -phenol,  $\text{CD}_3\text{OH}$ , and  $\text{CH}_3\text{OD}$  or  $\text{CD}_3\text{OD}$ . Both of the hydroxy groups of phenol and methanol are sufficiently acidic to allow for a rapid  $\text{H} \leftrightarrow \text{D}$  exchange, whereas the methyl group is virtually inert to this exchange. Isotopomers with different numbers of deuterium atoms can easily be distinguished by TOF mass spectrometry, as can be seen in Figure 1 for the undeuterated (trace a) and the doubly (trace c), three-fold (trace d), and five-fold (trace f) deuterated clusters. Single and four-fold deuteration leads to two different isotopomers. For one, the exchange takes place at the phenolic hydroxy group; for the other, at the methanolic  $-\text{OH}$  group. Their electronic origins can be distinguished by their spectral shifts. The electronic origins around  $35933 \text{ cm}^{-1}$  (see dashed line in Figure 1) belong to the deuteromethanol species, but the origins around  $35940 \text{ cm}^{-1}$  (solid line) can be attributed to the deuterophenol species, as can be deduced from comparisons to the undeuterated and fully deuterated clusters. By analyzing the different origins, it was

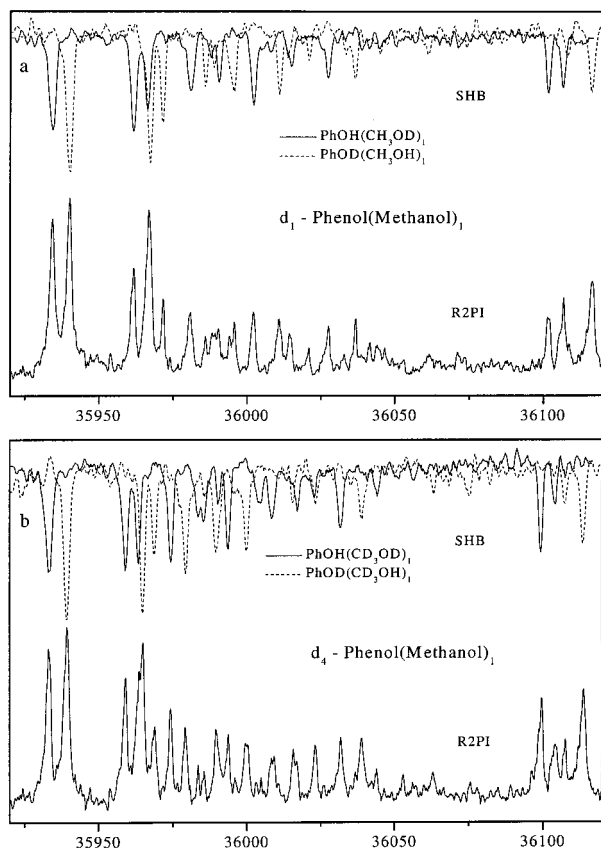


**Figure 2.** SHB spectra of the two  $d_1$  isotopomers of phenol–methanol (upper traces) (a) and of the two  $d_4$  isotopomers of phenol–methanol (upper traces) (b). The lower traces show the respective R2PI spectra.

possible to take SHB spectra of each of the isotopomers, which could not be separated in the TOF spectrometer. Figure 2 a and b present the hole-burning spectra of  $d_1$ - and  $d_4$ -phenol–methanol taken by probing the electronic origin of the deuteromethanol species and of the deuterophenol species, respectively. The experimental frequencies of the electronic origins and the corresponding vibronic transitions of all five isotopomers together with the vibrational assignments are collected in Table 1. The nomenclature for the assignments refers to the nomenclature in the phenol–water system given by Schütz et al.<sup>14</sup> Briefly, the six intermolecular vibrations are divided into two groups. One group describes the lost translational degrees of freedom of the methanol moiety along the  $x$ ,  $y$ , and  $z$  axes (cf. Figure 3) of the cluster ( $\sigma$ ,  $\beta_1$ ,  $\rho_1$ ); the other describes the lost rotational degrees of freedom about the inertial  $a$ ,  $b$ , and  $c$  axes of the methanol moiety ( $\beta_2$ ,  $\tau$ ,  $\rho_2$ ). The  $x$ -axis points in the direction of the hydrogen bond, whereas the  $z$ -axis is perpendicular to the aromatic ring. Figure 3 shows the structure of the cluster and the rotational and translational axes. Unfortunately, the assignment of the intermolecular modes in the phenol–methanol system to the lost degrees of freedom is not so straightforward as it is in case of the phenol–water system, which can be attributed to the fact that the methyl group of the methanol moiety is able to form a (van der Waals) bond toward the aromatic ring. This additional bond resists pure translational motions, and especially in the case of the  $\beta_1$  vibration, a considerable amount of methyl torsional motion mixes into the normal mode.

**B. Distinction of the Torsional Components.** After distinction of the isotopomers of phenol–methanol, the torsional components, which are due to the methyl group torsional motion, were studied using hole-burning spectroscopy. From high-

resolution LIF spectroscopy, the torsional splitting of the origin is known to be  $0.12 \text{ cm}^{-1}$  ( $3557.621 \text{ MHz}$ ).<sup>7</sup> This splitting is too small to allow for separate analysis of the two torsional components. As has been shown for the phenol–water cluster, the coupling of intermolecular vibrations with a large-amplitude motion might lead to splittings that are larger than those of the electronic origin.<sup>12</sup> In the case of phenol–methanol, possible candidates for strong coupling are the intermolecular vibrations, which comprise a considerable amount of methyl torsional motion. Figure 4 shows the SHB spectra of the undeuterated species obtained by analyzing the split vibronic bands at  $45.6$  and  $48.5 \text{ cm}^{-1}$ . Obviously, these bands belong to different ground-state levels and are assumed to be the torsional components of the wagging-mode  $\beta_2$ . The torsional splitting of the electronic origin is too small to be resolved (vide supra). The vibronic transition at  $70 \text{ cm}^{-1}$ , which is assigned to the  $\beta_1$  vibration, is split by  $0.8 \text{ cm}^{-1}$  (see Table 1), whereas the other vibronic bands have comparably small splittings as the origin. Both intermolecular modes  $\beta_1$  and  $\beta_2$  show a large extent of torsional character of the methyl group and, therefore, strong coupling to this large-amplitude internal motion.

From the analysis of the rotationally resolved LIF spectrum of phenol–methanol, the reduced barrier height  $V_3/F$  could be determined experimentally in the electronic ground and excited states to be  $32.16$  and  $27.65$ , respectively.<sup>7</sup> Assuming a 1-D methyl rotation, the internal rotation constant  $F$  was  $158.1$  and  $158.2 \text{ GHz}$  in the  $S_0$  and  $S_1$  states, respectively. With these internal rotation constants, one would calculate torsional barriers of  $170 \text{ cm}^{-1}$  in the electronic ground state and  $146 \text{ cm}^{-1}$  in the excited state. These values differ strongly from the  $V_3$  barrier in free methanol, which was determined to be  $376.8 \text{ cm}^{-1}$ .<sup>15</sup> A comparable reduction in barrier height upon cluster formation is known for other complexes of methanol. In the methanol dimer, the barrier to internal rotation in the acceptor methanol was determined to be  $120 \text{ cm}^{-1}$ ;<sup>16</sup> in the aniline–methanol cluster, the barrier was determined to be  $215 \text{ cm}^{-1}$ .<sup>17</sup> Fraser et al.<sup>18</sup> proposed that this decrease in barrier height is an artifact due to the coupling of the internal rotation to the librational motion of the methanol molecule about its inertial  $a$ -axis. This vibration is, in our case, the wagging-mode  $\beta_2$ . The large torsional splitting of this mode is a good indication of the correctness of this theory. Figure 5 shows the displacement vectors of the intramolecular torsion and the  $\beta_2$  mode. A contour plot of the potential energy surface along these two coordinates, calculated at the MP2/6-31G(d,p) level with all other internal coordinates fixed at their equilibrium values, is shown in Figure 6. Obviously, both motions are strongly coupled by anharmonic terms.

Using the reduced barrier heights from the high-resolution measurements,<sup>7</sup> we simulated a torsional spectrum of phenol–methanol. SHB analysis of the torsional components of the  $\beta_2$  mode should allow for an assignment of the pure torsional transitions to be made. Unfortunately, we were not able to identify any band in the spectra that was not a torsional component of a vibration. Therefore, the only information known about the torsional barrier is the A, E splitting of the electronic origin.<sup>8</sup>

**C. Intermolecular Vibronic Transitions.** The vibronic transitions, which are compiled in Table 1 for the  $d_0$ – $d_5$  isotopomers, are assigned by comparison to the results of ab initio calculations. As has been shown in ref 8, the intermolecular geometry of the cluster (e.g., the orientation of the phenol and the methanol moiety with respect to each other) can be reproduced satisfactorily at the CIS//6-31G(d,p) level of theory.

TABLE 1: Electronic Origins and Relative Vibronic Frequencies of  $d_n$ -Phenol–Methanol<sup>a</sup>

$d_0$	$d_1(m)^b$	$d_1(p)^b$	$d_2$	$d_3$	$d_4(m)$	$d_4(p)$	$d_5$	assignment <sup>c</sup>
0 (35 932.9)	0 (35 934.1)	0 (35 940.1)	0 (35 941.0)	0 (35 932.1)	0 (35 932.8)	0 (35 939.1)	0 (35 939.9)	0, 0
27.4	27.3	27.1	26.9	25.5	25.8	25.5	25.6	$\rho_2$
31.5	31.5	31.6	31.8	29.2	29.8	29.5	29.4	$\tau$
45.6 (A)	45.5 (A)	45.6 (A)	45.8 (A)					
48.5 (E)	46.9 (E)	48.6 (E)	47.0 (E)	39.6	40.6	39.8	39.4	$\beta_2$
53.7 (A)								
54.1 (E)	53.2	54.1	53.2	50.0	50.4	46.4	46.0	$\rho_1$
55.4	55.9	55.2	56.0		56.2	50.2	52.8	$2\rho_2$
70.0 (A)								
70.8 (E)	67.7	70.7	68.0	60.1	60.6	60.4	60.6	$\beta_1$
73.8	73.4	73.5		70.1	71.4	71.4	72.0	$\rho_2 + \beta_2$
80.6	79.8	80.7	80.4	76.2	75.5	76.0	75.8	$\rho_2 + \rho_1$
96.2	92.9	96.3	93.3	99.4	98.5	99.6	99.0	$\rho_2 + \beta_1$
120.4		120.7		123.6		124.3		$2\rho_2 + \beta_1$
168.3	167.4	167.7	167.4	168.0	166.6	168.1	167.1	twist <sup>d</sup>
176.6	172.2	176.0	171.3	174.4	170.3	174.1	169.7	$\sigma$

<sup>a</sup>  $n = 0-5$ . Relative uncertainty of the vibrational frequencies is  $0.2 \text{ cm}^{-1}$ . <sup>b</sup> (m) means deuteration in the methanol moiety; (p), deuteration in the phenol moiety. <sup>c</sup> Vibrational assignment according to the nomenclature of Schütz et al.<sup>14</sup> for the phenol–water system. <sup>d</sup> Intramolecular vibration localized in the phenol moiety.

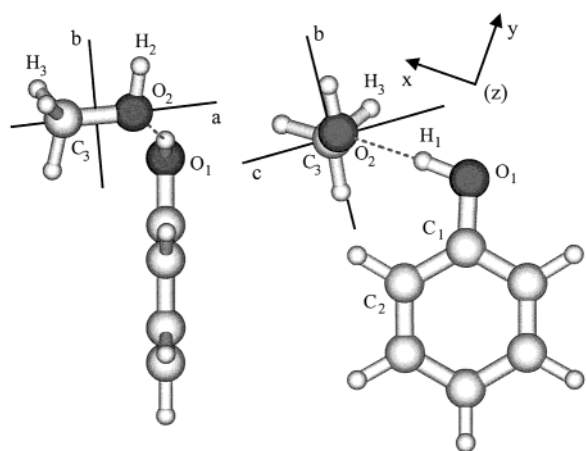


Figure 3. Structure of the phenol–methanol cluster and definitions of the axes of rotation and translation.

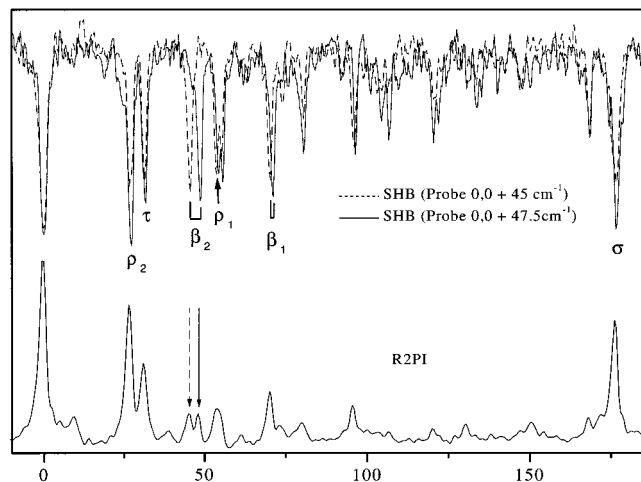


Figure 4. Hole-burning spectra of the torsional components of the phenol–methanol cluster (upper traces). The lower trace shows the R2PI spectrum with the analyzed transitions marked by arrows.

This geometry was confirmed not only for the rotational constants of the cluster but also for five intermolecular parameters that describe the orientation of the monomer units. Therefore, we attempted to assign the intermolecular vibrations on the basis of this calculation. Table 2 shows the calculated intermolecular vibrational frequencies. At first sight, the agree-

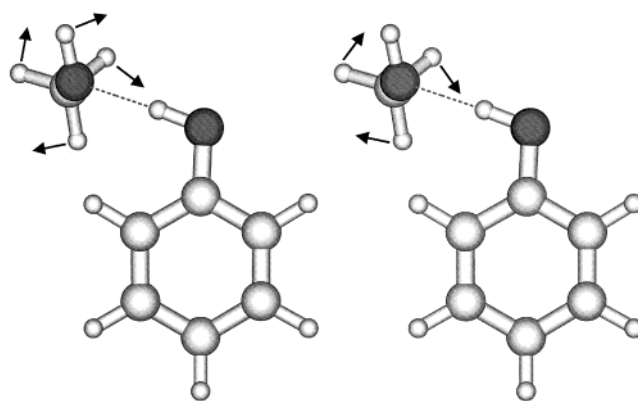


Figure 5. Schematic displacement vectors of the librational mode  $\beta_2$  and of the methyl torsional mode. The displacement vectors obtained from a normal-mode analysis at the MP2/6-31G(d,p) level show the displacements of the torsional motion as a torsion of the methanolic OH group about the rigid frame of the methanol moiety.

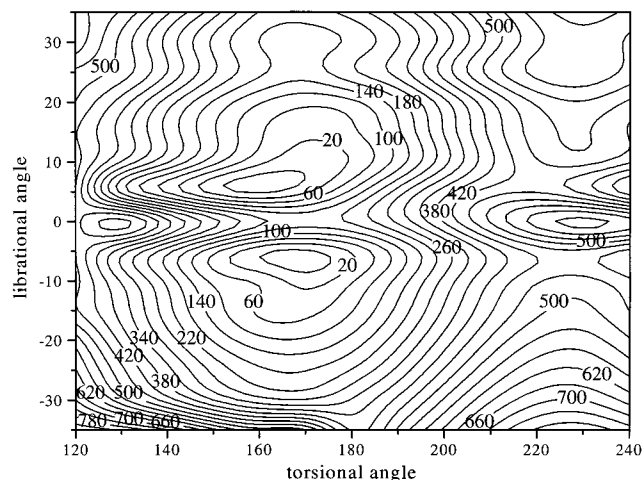


Figure 6. Intermolecular potential energy surface as function of the torsional angle  $\tau$  and the librational angle  $\beta_2$ .

ment of the frequencies with the experimental values seems to be very bad; therefore, we concentrated our efforts on the reproduction of the isotopic frequency shifts. Table 3 presents the calculated vibrational frequencies for the five isotopomeric clusters, scaled on the frequencies of the undeuterated cluster. The calculated frequency shifts show good agreement with the

**TABLE 2: Calculated Intermolecular  $S_1$  Vibrational Frequencies at the CIS//6-31G(d,p) Level of Theory**

mode	CIS//6-31G(d,p)							
	$d_0$	$d_1(m)$	$d_1(p)$	$d_2$	$d_3$	$d_4(m)$	$d_4(p)$	$d_5$
$\rho_2$	38.8	38.6	38.6	38.4	36.1	36.0	36.0	35.8
$\tau$	44.7	44.4	44.6	44.3	41.0	40.7	40.9	40.6
$\beta_2$	74.3	69.7	74.2	69.5	64.4	61.2	64.3	61.1
$\rho_1$	93.4	92.0	93.3	91.9	84.0	83.9	83.9	83.8
$\beta_1$	124.0	122.9	123.8	122.7	110.3	109.2	110.0	108.9
$\sigma$	177.6	171.1	177.0	170.4	173.8	168.1	173.2	167.4

experimental values given in parentheses in Table 3. On the basis of this data, together with the results of the analysis of torsional components in the spectra, we made the assignments given in the last column of Table 1.

The three lowest-frequency vibrations can be deduced from the rotation of the methanol moiety about its inertial  $c$  ( $\rho_2$ , 27.4  $\text{cm}^{-1}$ ),  $b$  ( $\tau$ , 31.5  $\text{cm}^{-1}$ ), and  $a$  ( $\beta_2$ , 45.6  $\text{cm}^{-1}$ ) axes. The  $\beta_2$  vibration is split into its A and E torsional components (cf. Figure 4) so that the band at 48.5  $\text{cm}^{-1}$  must be attributed to the E torsional component of this vibration. In a previous publication,<sup>5</sup> this band was assigned to the  $\rho_1$  vibration, which could be disproved by the present investigation. Similar splitting can be observed for the  $d_1$  and  $d_2$  isotopomers as well, although in these cases the possibility that these isotopomers have different torsional components has not been proven by SHB. Because of the much smaller torsional constants for  $d_3$ - to  $d_5$ -phenol-methanol, splitting is not observed for these isotopomers.

The next three intermolecular vibrations are of translational parentage. The first ( $\rho_1$ ) is due to the lost translational degree of freedom along the  $z$ -axis, which is perpendicular to the aromatic ring. Although the calculated frequency deviates considerably from the experimental value, the transition at 53.7  $\text{cm}^{-1}$  ( $d_0$ ) has been assigned to this vibration on the basis of the isotopic shifts. This band shows a small splitting of 0.4  $\text{cm}^{-1}$ , which can be attributed to the torsional A, E splitting. The transition at 55.4  $\text{cm}^{-1}$  fits to the overtone of the  $\rho_2$  vibration (27.4  $\text{cm}^{-1}$ ) and fits similarly well for the other isotopomers. The torsional splitting of this overtone is comparably small to that of the fundamental and could not be resolved.

The transition at 70  $\text{cm}^{-1}$  again shows torsional splitting, which is larger in this case (0.8  $\text{cm}^{-1}$ ). The frequency pattern of the isotopomers allows the assignment of this band to the  $y$ -axis translational mode ( $\beta_1$ ). As has been argued before, the form of the normal mode is much more complex than just a simple translational motion but shows a considerable amount of methyl torsion, which explains the larger splitting for this mode. In a previous publication,<sup>5</sup> the  $\beta_1$  vibration was assigned to a transition at 96  $\text{cm}^{-1}$ .

The band at 73.8  $\text{cm}^{-1}$  can be assigned to a combination band  $\rho_2 + \beta_2$  that fits equally well for all isotopomers, whereas the transition at 80.6  $\text{cm}^{-1}$  can be attributed to the combination band  $\rho_2 + \rho_1$  and 96.2  $\text{cm}^{-1}$ , to  $\rho_2 + \beta_1$ .

The remaining stretching vibration  $\sigma$  can be assigned to the transition at 176.6  $\text{cm}^{-1}$  from the absolute calculated frequency as well as from the isotopic pattern.

One transition at 168.3  $\text{cm}^{-1}$  remains, which could not be assigned to an intermolecular vibration. This band shows virtually no isotopic shift, contrary to all other observed transitions. It therefore cannot be explained by a combination or overtone band, so we believe that this transition can be assigned to an intramolecular vibration. The only vibration in this frequency range attributable to our calculations is the twisting motion of the phenyl ring. Its frequency in the cluster

is calculated to be 231  $\text{cm}^{-1}$ . Because of the fact that for the three vibrations  $\beta_2$ ,  $\rho_1$ , and  $\beta_1$  the harmonic motion has considerable torsional components, another alternative assignment for these three vibrations has to be considered. A least-squares fit of all of the (scaled) intermolecular frequencies of the isotopomers to the calculated isotopic shifts gave better agreement if  $\beta_2$  and  $\beta_1$  are interchanged. This result cannot be completely excluded, because each of these vibrations might show considerable torsional splitting. Nevertheless, with this assignment, the  $\beta_1$  vibration, which had been calculated (in the harmonic approximation) to be 124  $\text{cm}^{-1}$ , is observed at 45.6  $\text{cm}^{-1}$ . Although large deviations due to anharmonicity are found in these clusters, this difference seems rather large.

**D. Dispersed Fluorescence Spectra and Intermolecular Ground-State Vibrations.** The mass-selective R2PI and species-selective hole-burning experiments showed that four isotopomers of phenol-methanol can easily be examined via dispersed fluorescence spectroscopy. The  $d_0$ ,  $d_2$ ,  $d_3$ , and  $d_5$  spectra consist of only one isotopomer and can therefore be excited selectively. Dispersed fluorescence spectra of  $d_0$  and  $d_5$  together with a vibrational assignment have already been presented.<sup>5</sup> Figure 7 shows the dispersed fluorescence spectrum of  $d_2$ -phenol-methanol obtained by pumping the electronic origin at 35 941.0  $\text{cm}^{-1}$  (a),  $d_3$ -phenol-methanol obtained by exciting the electronic origin at 35 932.1  $\text{cm}^{-1}$  (b), and the  $\rho_2$  vibration of  $d_3$ -phenol-methanol at 0.0 + 25.5  $\text{cm}^{-1}$  (c). The fluorescence intensity of the  $d_2$  isotopomer is much weaker than that of  $d_3$ -phenol-methanol. The vibrational frequencies of the  $d_2$  and  $d_3$  isotopomers together with the  $d_0$  and  $d_5$  frequencies from publication<sup>5</sup> are compiled in Table 4. The frequencies of the additional measured isotopomeric clusters fit well into the isotopic pattern of the  $d_0$  and  $d_5$  isotopomers.

The vibrational frequencies for the electronic ground state have been calculated at the MP2//6-31G(d,p) level of theory and have been compared to frequencies calculated at the HF//6-31G(d,p) level. The resulting vibrational frequencies are given in Tables 5 and 6. As for assignments made for the  $S_1$  state, the assignment of the vibrational frequencies is based upon the comparison to the scaled vibrational frequencies of *all* isotopomers. The only severe deviation concerns the  $\beta_1$  vibration, which might be caused by strong coupling to the methyl torsion and the resulting large anharmonicity.

In contrast to that in the  $S_1$  state, the assignment of the intermolecular vibrations in the  $S_0$  state is identical to the assignment given in ref 5. As a matter of fact, the vibrational frequencies calculated at the HF level of theory are more accurate with respect to the absolute value, as well as to the isotopic pattern, than are the MP2 frequencies. Regarding the fact that the experimental geometry of the cluster can be reproduced well at MP2 level whereas HF as well as DFT methods clearly fail,<sup>7,8</sup> the reliability of structural determinations from the comparison of experimental vibrational frequencies to the results of ab initio-based normal-mode analysis must be doubted, at least for more complex cases.

## V. Conclusions

A vibrational assignment of the intermolecular vibrations of the phenol-methanol cluster could be given for the electronic ground and first excited states by comparing the results of an ab initio normal-mode analysis with the experimental frequencies of five isotopically substituted phenol-methanol clusters. The  $\beta_2$  and  $\beta_1$  vibrations show a torsional splitting that is considerably larger than that for any other vibration. The torsional components could be separated using hole-burning

**TABLE 3: Calculated  $S_1$  Vibrational Frequencies for Five Isotomers of Phenol–Methanol<sup>a</sup>**

CIS//6-31G(d,p) scaled								
mode	$d_0$	$d_1(m)$	$d_1(p)$	$d_2$	$d_3$	$d_4(m)$	$d_4(p)$	$d_5$
$\rho_2$	27.4	27.3 (27.3)	27.3 (27.1)	27.1 (26.9)	25.5 (25.5)	25.4 (25.8)	25.4 (25.5)	25.3 (25.6)
t	31.5	31.3 (31.5)	31.4 (31.6)	31.2 (31.8)	28.9 (29.2)	28.7 (29.8)	28.8 (29.5)	28.6 (29.4)
$\beta_2$	45.6	42.8 (45.5)	45.5 (45.6)	42.7 (45.8)	39.5 (39.6)	37.6 (40.6)	39.5 (39.8)	37.5 (39.4)
$\rho_1$	54.0	53.2 (53.2)	53.9 (54.1)	53.1 (53.2)	48.6 (50.0)	48.5 (50.4)	48.5 (46.4)	48.4 (46.0)
$\beta_1$	70.3	69.7 (67.7)	70.2 (70.7)	69.6 (68.0)	62.5 (60.1)	61.9 (60.6)	62.4 (60.4)	61.7 (60.6)
$\sigma$	176.6	170.1 (172.2)	176.0 (176.0)	169.4 (171.3)	172.8 (174.4)	167.2 (170.3)	172.2 (174.1)	166.5 (169.7)

<sup>a</sup>Values have been scaled to the experimental frequencies of the undeuterated isotopomer, and the resulting scaling factors have been used to correct the calculated frequencies from Table 2. Experimental values are given in parentheses.

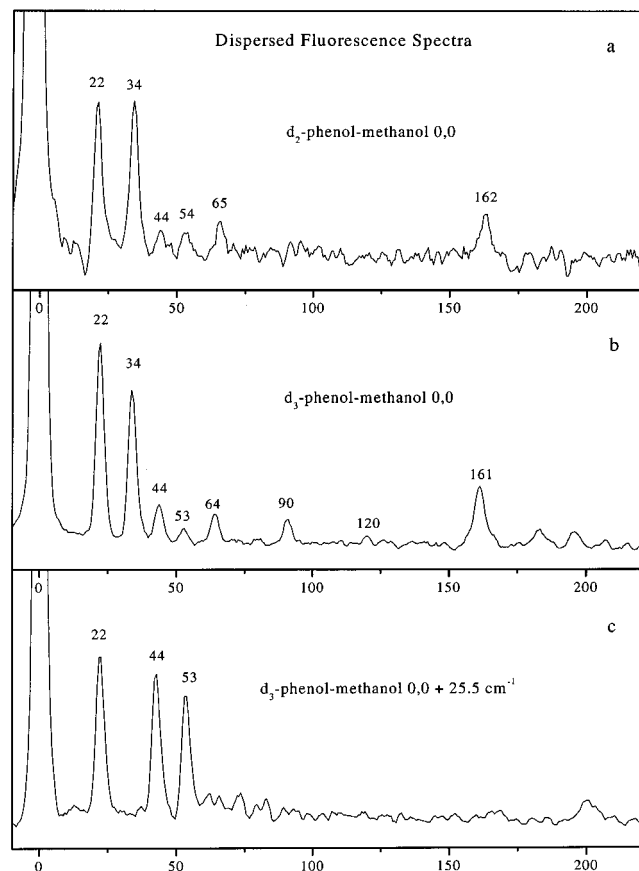


**Figure 7.** Dispersed fluorescence spectra of  $d_2$ -phenol–methanol obtained by exciting the electronic origin (a), of  $d_3$ -phenol–methanol obtained by exciting the electronic origin (b), and of the  $\rho_2$  vibronic band at  $0.0 + 25.5 \text{ cm}^{-1}$  (c). The DF spectrum of  $d_2$ -phenol–methanol is recorded with an entrance slit width of  $100 \mu\text{m}$  compared to that of  $50 \mu\text{m}$  for the  $d_3$  isotopomer because of the much weaker signal.

**TABLE 4: Relative Vibrational Frequencies of the Electronic Ground State of  $d_0$ -,  $d_2$ -,  $d_3$ -, and  $d_5$ -Phenol–Methanol**

$d_0^a$	$d_2$	$d_3$	$d_5^a$	assignment <sup>b</sup>
22	22	22	22	$\rho_2$
35	34	34	33	t
55	53	44	42	$\beta_2$
65	65	64	64	$\rho_1$
91		90	90	$\beta_1$
162	162	161	155	$\sigma$

<sup>a</sup>Frequencies of  $d_0$  and  $d_5$  moieties are taken from ref 5. <sup>b</sup>Vibrational assignment according to the nomenclature of Schütz et al.<sup>14</sup> for the phenol–water system.

spectroscopy with analysis of the A and E subbands of the  $\beta_2$  vibration, which is split by  $2.9 \text{ cm}^{-1}$ . The large splitting of this vibration in comparison to the splitting of the origin ( $0.1 \text{ cm}^{-1}$ )

**TABLE 5: Calculated Intermolecular  $S_0$  Vibrational Frequencies at the HF//6-31G(d,p) Level of Theory**

HF//6-31G(d,p)								
mode	$d_0$	$d_1(m)$	$d_1(p)$	$d_2$	$d_3$	$d_4(m)$	$d_4(p)$	$d_5$
$\rho_2$	17.3	17.1	17.2	17.0	16.0	15.9	15.9	15.8
$\tau$	30.2	30.1	30.1	29.9	28.1	27.9	27.9	27.8
$\beta_2$	54.6	51.1	54.5	51.0	43.0	41.5	43.0	41.5
$\rho_1$	70.3	70.2	70.3	70.2	67.3	67.1	67.3	67.1
$\beta_1$	90.4	89.1	90.2	88.9	82.5	81.0	82.3	80.8
$\sigma$	158.1	152.8	157.3	152.1	155.5	150.5	154.7	149.7

**TABLE 6: Calculated Intermolecular  $S_0$  Vibrational Frequencies at the MP2//6-31G(d,p) Level of Theory**

MP2//6-31G(d,p)								
mode	$d_0$	$d_1(m)$	$d_1(p)$	$d_2$	$d_3$	$d_4(m)$	$d_4(p)$	$d_5$
$\rho_2$	38.0	37.7	37.9	37.6	36.0	35.8	35.9	35.8
$\tau$	60.3	60.3	60.1	60.1	55.5	55.5	55.3	55.5
$\beta_2$	80.7	75.7	80.6	75.6	68.5	65.6	68.4	65.6
$\rho_1$	102.7	102.5	102.7	102.4	94.0	93.6	94.0	93.6
$\beta_1$	140.6	139.1	140.4	138.9	121.1	119.7	120.9	119.7
$\sigma$	199.1	192.5	198.5	191.8	194.6	189.0	194.0	189.0

**TABLE 7: Calculated  $S_0$  Vibrational Frequencies for Five Isotomers of Phenol–Methanol<sup>a</sup>**

scaled							
mode	HF/MP, $d_0$	HF, $d_2$	MP2, $d_2$	HF, $d_3$	MP2, $d_3$	HF, $d_5$	MP2, $d_5$
$\rho_2$	22	21.5	21.7 (22)	20.3	20.8 (22)	20.0	20.7 (22)
$\tau$	35	34.6	34.9 (34)	32.6	32.2 (34)	32.2	32.2 (33)
$\beta_2$	55	51.4	51.5 (53)	43.3	46.7 (44)	41.8	44.7 (42)
$\rho_1$	65	64.9	64.8 (65)	62.2	59.5 (64)	62.0	59.2 (64)
$\beta_1$	91	89.5	89.9	83.0	78.4 (90)	81.3	77.5 (90)
$\sigma$	162	155.8	156.0 (162)	159.3	158.3 (161)	153.4	153.8 (155)

<sup>a</sup>Values have been scaled to the experimental frequencies of the undeuterated isotopomer, and the resulting scaling factors have been used to correct the calculated frequencies from Tables 5 and 6. Experimental values are given in parentheses.

can be explained by the strong coupling of the  $\beta_2$  mode to the methyl torsion in the  $S_1$  state.

Although the absolute vibrational frequencies at the CIS level for the  $S_1$  state and at the MP2 level for the  $S_0$  state show large deviations from the experimental values, assignments could be made by utilizing both the isotopic pattern and the information from the torsional splitting. Using the same level of theory and the same basis set, we were able to reproduce the experimental intermolecular geometry of the cluster quite well. Nevertheless, the CIS method exhibits severe discrepancies concerning the dispersive interaction between the methyl group and the aromatic ring. The uncommonly high scaling factors for the vibrational frequencies are probably caused by errors due to the harmonic approximation. Deviations in the isotopic pattern point to deficiencies in the description of the intermolecular potential at the CIS level. Whereas the description of the electronic ground state with a single determinant method leads to the wrong

intermolecular geometry, the CIS method at least yields a geometry that is in accordance with the experimental one. Nevertheless, correct descriptions of the geometry and intermolecular potential can be expected only by using a perturbative approach like CASPT2 (Table 7).

**Acknowledgment.** We especially thank Professor Kleiner-manns for his steady interest in this work and for many helpful discussions. The help of Petra Imhof with the DF measurements is gratefully acknowledged. Thanks to Professor Weinkauff for making available to us his LPX 100. We thank the Deutsche Forschungsgemeinschaft for financial support of this work. This work is part of the dissertation of Ch.P.

## References and Notes

- (1) Abe, H.; Mikami, N.; Ito, M. *J. Phys. Chem.* **1982**, *86*, 1768.
- (2) Abe, H.; Mikami, N.; Ito, M.; Udagawa, Y. *J. Phys. Chem.* **1982**, *86*, 2567.
- (3) Wright, T. G.; Cordes, E.; Dopfer, O.; Müller-Dethlefs, K. *J. Chem. Soc., Faraday Trans.* **1993**, *89*, 1601.
- (4) Gerhards, M.; Beckmann, K.; Kleiner-manns, K. *Z. Phys D: At., Mol., Clusters* **1994**, *29*, 223.
- (5) Schmitt, M.; Müller, H.; Henrichs, U.; Gerhards, M.; Perl, W.; Deusen, C.; Kleiner-manns, K. *J. Chem. Phys.* **1995**, *103*, 584.
- (6) Courty, A.; Mons, M.; Dimicoli, B.; PiuZZi, F.; Brenner, V.; Millié, P. *J. Phys. Chem. A* **1998**, *102*, 4890.
- (7) Schmitt, M.; Küpper, J.; Spangenberg, D.; Westphal, A. *Chem. Phys.* **2000**, *254*, 349.
- (8) Küpper, J.; Westphal, A.; Schmitt, M. *Chem. Phys.* **2001**, *263*, 41.
- (9) Gudladt, U. Mikrowellenspektroskopische Untersuchungen des Komplexes Phenol–Methanol. M.S. Thesis, Christian Albrechts Universität, Kiel, 1996.
- (10) Frisch, M. J.; Trucks, G. W.; Schlegel, H. B.; Scuseria, G. E.; Robb, M. A.; Cheeseman, J. R.; Zakrzewski, V. G.; Montgomery, J. A., Jr.; Stratmann, R. E.; Burant, J. C.; Dapprich, S.; Millam, J. M.; Daniels, A. D.; Kudin, K. N.; Strain, M. C.; Farkas, O.; Tomasi, J.; Barone, V.; Cossi, M.; Cammi, R.; Mennucci, B.; Pomelli, C.; Adamo, C.; Clifford, S.; Ochterski, J.; Petersson, G. A.; Ayala, P. Y.; Cui, Q.; Morokuma, K.; Malick, D. K.; Rabuck, A. D.; Raghavachari, K.; Foresman, J. B.; Cioslowski, J.; Ortiz, J. V.; Stefanov, B. B.; Liu, G.; Liashenko, A.; Piskorz, P.; Komaromi, I.; Gomperts, R.; Martin, R. L.; Fox, D. J.; Keith, T.; Al-Laham, M. A.; Peng, C. Y.; Nanayakkara, A.; Gonzalez, C.; Challacombe, M.; Gill, P. M. W.; Johnson, B. G.; Chen, W.; Wong, M. W.; Andres, J. L.; Head-Gordon, M.; Replogle, E. S.; Pople, J. A. *Gaussian 98*, revision A.7; Gaussian, Inc.: Pittsburgh, PA, 1998.
- (11) Lommatzsch, U.; Brutschy, B. *Chem. Phys.* **1998**, *234*, 35.
- (12) Schmitt, M.; Jacoby, C.; Kleiner-manns, K. *J. Chem. Phys.* **1998**, *108*, 4486.
- (13) Roth, W.; Jacoby, C.; Westphal, A.; Schmitt, M. *J. Phys. Chem. A* **1998**, *102*, 3048.
- (14) Schütz, M.; Bürgi, T.; Leutwyler, S.; Fischer, T. *J. Chem. Phys.* **1993**, *98*, 3763.
- (15) Gerry, M. C. L.; Lees, R. M.; Winnewisser, G. *J. Mol. Spectrosc.* **1976**, *61*, 231.
- (16) Lovas, F. J.; Belov, S. P.; Tretyakov, M. Y.; Stahl, W.; Suenram, R. D. *J. Mol. Spectrosc.* **1995**, *170*, 478.
- (17) Haeckel, M.; Stahl, W. *J. Mol. Spectrosc.* **1999**, *198*, 263.
- (18) Fraser, G. T.; Lovas, F. J.; Suenram, R. D. *J. Mol. Spectrosc.* **1994**, *167*, 231.